

# ENERGY VERIFICATION IN ION BEAM THERAPY \*

F. Moser<sup>†</sup>, M. Benedikt, CERN, Geneva, Switzerland  
 U. Dorda, EBG MedAustron, Wr. Neustadt, Austria

## Abstract

The adoption of synchrotrons for medical applications necessitates a comprehensive on-line verification of all beam parameters, autonomous of common beam monitors. In particular for energy verification, the required precision of down to 0.1 MeV in absolute terms, poses a special challenge regarding the betatron-core driven 3rd order extraction mechanism which is intended to be used at MedAustron [1]. Two different energy verification options have been studied and their limiting factors were investigated: 1) A time-of-flight measurement in the synchrotron, limited by the orbit circumference information and measurement duration as well as extraction uncertainties. 2) A calorimeter-style system in the extraction line, limited by radiation hardness and statistical fluctuations. The paper discusses in detail the benefits and specific aspects of each method.

## INTRODUCTION

Ion beam therapy is a method of treating cancer patients by application of a homogeneous dose field aimed at irreversibly damaging the tumour cells. The depth-profile of such a dose field is determined by the energy of the impinging particles. Incorrect energies can cause unintended damage of healthy tissue and dose inhomogeneities inside the target region resulting in increased survival probability for tumour cells. Energy verification aims at reducing the risk associated with these problems. If implemented in concert with commonly used verification of beam intensity, profile and position, energy verification removes all assumptions about beam properties and paves the way for the usage of general-purpose (as opposed to medical-purpose) accelerators as “beam suppliers”. Published cases of energy verification report either similar precision to the 0.1 MeV mentioned in the abstract [3] or inferior precision [4, 5].

The energy verification methods presented in the following are universal, but to allow for quantitative evaluation, the performance figures have been tailored for the MedAustron synchrotron, which is based on the design proposed by the Proton-Ion Medical Machine Study (PIMMS) [2]. Unlike other medical synchrotrons, PIMMS proposes the usage of induction acceleration as driving mechanism for the 3rd order slow resonant extraction. This implies slight acceleration of the unbunched beam before extraction. Therefore the time-of-flight measurement discussed in the following section can not measure the energy

of the extracted beam, but measures the beam energy before debunching.

## TIME-OF-FLIGHT MEASUREMENT

The measurement of the beam energy by means of a time-of-flight measurement is based on the equation for the kinetic energy of a single particle<sup>1</sup>:

$$E_{\text{kin}} = mc^2 \left( \frac{1}{\sqrt{1 - C^2 f^2 / c^2}} - 1 \right) \quad (1)$$

with the particle mass  $m$ , the orbit circumference  $C$ , the revolution frequency  $f$  and the speed of light  $c$ . A synchronous measurement of the closed orbit circumference and the bunch revolution frequency can be used for energy verification. Because the bunch must rotate on a fixed orbit during the measurement, it can be performed only in synchrotrons.

### Orbit circumference

The circumference of the closed orbit in a synchrotron is a function of the circumference of the reference orbit<sup>2</sup> and the transverse displacement of the closed orbit with respect to the reference orbit. The circumference of the reference orbit  $C_0$  depends only on constant parameters like the geometry and alignment of the lattice magnets. The associated uncertainty can be eliminated by repeated measurements during commissioning.

Once the transverse displacement of the closed orbit is measured, the circumference  $C$  of the displaced orbit can be computed on-line from  $C_0$  and the measured transverse displacements. To evaluate the uncertainty of the circumference, MAD-X simulations have been performed for the MedAustron machine, taking into account lattice errors (alignment errors of  $\sigma = 0.3$  mm and field errors as specified in the PIMMS) and a limited beam position monitor precision of  $\sigma_{xy} = 0.4$  mm for all eleven horizontal ( $Q_x \approx 1.67$ ) and eight vertical ( $Q_y \approx 1.79$ ) beam monitors. The resulting standard deviation of the reconstructed closed orbit circumferences evaluates to  $\sigma_C = 0.54$  mm. It is noteworthy that this value increases by up to an order of magnitude, depending on which monitor fails, if only one beam position monitor is unavailable.

<sup>1</sup>Although this does not strictly hold for averaged “beam” properties due to Jensen’s inequality  $E_{\text{kin}}(\langle Cf \rangle) \leq \langle E_{\text{kin}}(Cf) \rangle$  [6], an upper limit of the relative energy shift introduced by such an approximation can be shown to be two orders of magnitude smaller than the required energy precision, i.e.  $\mathcal{O}(10^{-5})$ .

<sup>2</sup>The reference orbit is (arbitrarily) defined by the operator based on closed orbit measurements; in general it is not the same as the design orbit.

\*Work supported by the Austrian Federal Ministry for Science and Research within the CERN Technology Doctoral Student Program

<sup>†</sup>fabian.moser@cern.ch

### Bunch revolution frequency

In order to rely only on independent straightforward measurements, the revolution frequency is derived from the signal of a wide-band beam pick-up and not taken from the low-level RF electronics. If that signal is at least twice oversampled, the uncertainty of the computed frequency resulting from a Fourier transform of the samples is the inverse of the record length. To achieve the required energy verification precision in the MedAustron synchrotron ( $C \approx 78$  m), the sampling frequency must be above 4.8 MHz for a 250 MeV proton beam or above 5.6 MHz for a 400 MeV/u carbon beam. For the closed orbit circumference uncertainty given above, the record length for the frequency measurement must be above 1.6 ms or above 5.6 ms for high-energy protons or carbon ions respectively.

## CALORIMETRIC MEASUREMENT

In contrast to the time-of-flight measurement described above, which is carried out in the synchrotron and based on measurements of collective “beam” properties, the measurement described here is carried out in the high-energy transfer line and exploits single-particle properties. While it is similar to calorimeters commonly used in high-energy physics experiments, there are two differences which clearly differentiate it:

- All particles hit the detector effectively at the same position and under the same angle because they originate from a beam rather than a collision or a decay.
- The measurement result is not an energy, but a decision whether a given set of data indicates a correct or an incorrect ion beam energy.

In the following it will be shown, that these two basic differences require reconsideration of some common calorimetry concepts.

### Mechanical integration and radiation hardness

At the start of each spill, the beam is always directed onto a beam dump which is equipped with beam profile and intensity monitors to qualify the beam upon extraction [2] (see figure 1). It is proposed to replace parts of this dump by the detector arrangement explained in the next subsection.

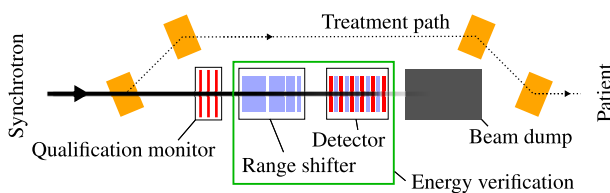


Figure 1: Conceptual integration scheme with the chopper dump region.

The annual dose deposited on the chopper dump has been estimated from the foreseen irradiation scenarios to

1 MGy on the surface with a rapid fall-off to about 0.2 MGy within the first two centimetres due to transverse straggling. This minimum is followed by a local maximum of 0.5 MGy about 10 cm inside the dump due to the Bragg peak of the involved dose curves. Beyond a depth of 40 cm the observed dose drops to a negligible level. Detectors known to withstand such radiation levels are ionisation chambers and diamond detectors, the latter being superior in terms of energy resolution.

### Conceptual design

The design of the proposed detector resembles that of a sampling calorimeter in that it consists of alternating active and passive layers. The active layers consist of chemical vapour deposited (CVD) diamond. Their thickness is chosen to be 0.5 mm to conform with off-the-shelf components. The passive layers consist of acrylic glass (PMMA), which is a common energy moderator in hadron therapy due to its similarity to human body with respect to its effect on ion beams. Simulations found that a thickness of 1.0 mm achieves an optimal balance between performance and dynamic range of the detector when the number of active layers is held constant.

In order to use fewer expensive active layers, the detector is preceded by a range shifter made of PMMA absorbers of different thickness that can be slowly moved in and out of the beam path. Optimisation showed that the best balance between the number of active layers and the necessary range shifter steps is achieved with four active layers and six passive blocks of different thickness allowing for 64 equally spaced range shifter steps. Using this design, the expected radiation dose in the first two active layers is approximately 90 kGy, which allows for long replacement periods of the active detector layers (in the order of a few years).

### Processing

The decision taking whether a recorded sample is accepted or rejected is based on a hypothesis test against a reference sample for the expected energy obtained during commissioning. The samples consist of a certain number of events, where each event contains the per-layer energy deposit generated by a single particle (and secondary particles). The comparison is based on an extension of the Wilcoxon-Mann-Whitney test, a robust non-parametric multivariate hypothesis test [7] which has been chosen after a benchmark including Hotelling's  $T^2$  test and multivariate extensions of the Kolmogorov-Smirnov test and Kuiper's test.

### Simulation & evaluation

The described detector design has been developed through iterative simulations with Geant4 [8]. The employed physics list was QGSP\_BIC\_EMY, which has been designed and tested specifically to address simulation problems of this kind [9].

The detector response is modelled outside of Geant4 by multiplication of the deposited energy with the mean electron-hole generation energy while taking the typical charge collection efficiency of the simulated detector into account [10]. The noise expected from the electronic signal amplification is modelled in terms of energy equivalent noise with a standard deviation of 10 keV. A lower amplifier threshold is assumed at an energy equivalent of 40 keV.

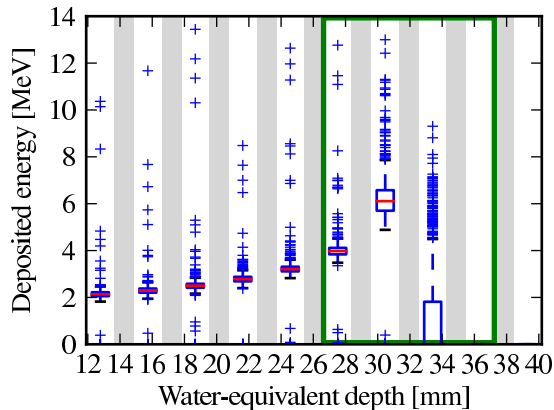


Figure 2: Result of a Geant4 simulation of 1000 particles from a 60 MeV proton beam. The plot shows the energy deposited by each particle in a stack of alternating active (white) and passive (grey) layers. Only the four active layers inside the green frame are used for processing. The other ones are displayed for illustration purposes only. The boxes in each active layer indicate the inter-quartile distances with the medians indicated by the red lines. The medians follow a Bragg-curve shape, increasing with depth.

An exemplary simulation result is shown in figure 2 which illustrates the distribution of the single-particle signals in each layer. The results match the expected Landau distribution for energy deposition in thin layers.

The energy verification performance has been evaluated using independently generated reference and test samples (using different seeds for the Geant4 random generator). At a statistical significance of 2.7‰ (equivalent to a “3 $\sigma$ ” confidence level for a normal distribution), the probability to reject an energy offset of 0.1 MeV of a 60 MeV proton beam (statistical power) is above 99.99%.

### Continuous energy verification

The methods presented so far measure the beam energy for each cycle prior to the patient irradiation, but not during the irradiation. However, only an on-line verification during the treatment would provide a similar level of supervision of the beam energy as is achieved for beam intensity, profile and position. It would cover an even wider range of possible errors, even though the likelihood of a change in energy of the extracted beam during extraction is low. An on-line measurement has already been recommended by the ICRU [11, section 2.4].

## 06 Beam Instrumentation and Feedback

### T03 Beam Diagnostics and Instrumentation

Simulations similar to the one described above for the chopper dump have been performed with the detector being positioned such that it intercepts beam halo particles during the course of the treatment. Preliminary simulation results suggest the feasibility of such a measurement. The main challenge for an on-line verification is the required significance to avoid reliability degradation of the overall operation i.e. too many unnecessary treatment interruptions, while decreasing the total beam intensity as little as possible.

## CONCLUSION

Both of the presented methods are capable of performing energy verification at the desired precision. As illustrated, the time-of-flight measurement can only verify the correctness of the RF acceleration, but not the final energy of the extracted particles. The calorimetric measurement in the high energy beam transfer line does not have this disadvantage. However, the performance of this second method has yet to be experimentally verified.

## REFERENCES

- [1] M. Benedikt and A. Wrulich, “MedAustronProject overview and status,” *Eur. Phys. J. Plus*, vol. 126, no. 7, Jul. 2011.
- [2] P.J. Bryant, et al., *Proton-Ion Medical Machine Study*, vol. 2, 2 vols. Geneva: CERN, 2000.
- [3] M. T. Gillin et al., “Commissioning of the discrete spot scanning proton beam delivery system at the University of Texas M.D. Anderson Cancer Center, Proton Therapy Center, Houston,” *Medical Physics*, vol. 37, no. 1, pp. 154-163, Jan. 2010.
- [4] E. Pedroni, et al., *Conceptual design of a new compact scanning gantry for proton therapy*, Villigen: Paul Scherrer Institute, 2004.
- [5] M.F. Moyers, et al., “Calibration of a proton beam energy monitor,” *Med. Phys.*, vol. 34, no. 6, pp. 1952-1966, Jun. 2007.
- [6] J.L.W.V. Jensen, “Sur les fonctions convexes et les inégalités entre les valeurs moyennes,” *Acta Math.*, vol. 30, no. 1, pp. 175-193, Dec. 1906.
- [7] R.R. Wilcox, *Introduction to robust estimation and hypothesis testing*, Amsterdam: Elsevier, 2005.
- [8] S. Agostinelli, “GEANT4: A Simulation toolkit,” *Nucl. Instrum. Meth. A*, vol. 506, no. 3, pp. 250-303, Jul. 2003.
- [9] G.G.P. Cirrone, et al., “Hadrontherapy: An open source, Geant4-based application for proton-ion therapy studies,” in *2009 IEEE Nuclear Science Symposium Conference Record (NSS/MIC)*, 2009, pp. 4186-4189.
- [10] H. Pernegger, private communication, CERN, Jan. 7, 2011
- [11] International Commission on Radiation Units, Measurements, and International Atomic Energy Agency, *Prescribing, recording and reporting proton-beam therapy*, vol. 2, Oxford: Oxford University Press, 2007.